Electronic Supplementary Material (ESI) for RSC Advances.

Supplementary Information for:

Wavelength-dependent photoconductivity of single-walled carbon nanotube layers

Serguei Smirnov,[a] Ilya V. Anoshkin,[b] Andrey Generalov,[c] Dmitri V. Lioubtchenko,[a] Joachim Oberhammer[a]*

[a] Department of Micro and Nanosystems, KTH Royal Institute of Technology, Malvinas väg 10, SE-100 44, Stockholm, Sweden.

[b] Department of Photonics and Optical Information Technologies, ITMO University, 49 Kronverkskiy pr., 197101 Saint Petersburg, Russian Federation.

[c] Department of Electronics and Nanoengineering, Aalto University, P.O. Box 13500 FI-00076, Finland.

*E-mail: dml@kth.se

Table S1. Fit parameters for S_{11} absorbance peaks and calculated nanotube diameter distribution. E_i are the centers of the peaks, w_i the weighting coefficients, and d the calculated nanotube diameter according to [1].

E_i [eV]	w_i	d [nm]
0.57	0.02	1.88
0.65	0.04	1.68
0.73	0.12	1.48
0.79	0.18	1.36
0.47	0.14	1.23
0.95	0.13	1.12
1.02	0.10	1.01
1.09	0.09	0.87

Table S2. Power levels of the lasers at different attenuation levels.

Wavelength [nm]		488	514	633	785
Power at	0 dB [mW]	22	28	17	56
	-3 dB	11	14	8.5	28
	-6 dB	5.5	7	4.25	14
	-10 dB	2.2	2.8	1.7	5.6
	-20 dB	0.22	0.28	0.17	0.56
	-30 dB	0.022	0.028		

Table S3. Fit parameters for the RBM peaks in the Raman spectrum and corresponding nanotube diameters calculated according to $\omega_{RBM} = 217.8/d + 15.7$ [2].

ω_{RBM} [cm^{-1}]	Γ_{RBM} [cm^{-1}]	d [nm]
122.6	11.5	2.0
138.1	15.3	1.8
165.8	10.5	1.5
183.1	8.7	1.3
192.2	14.2	1.2
215.7	7.6	1.1
253.7	10	0.9

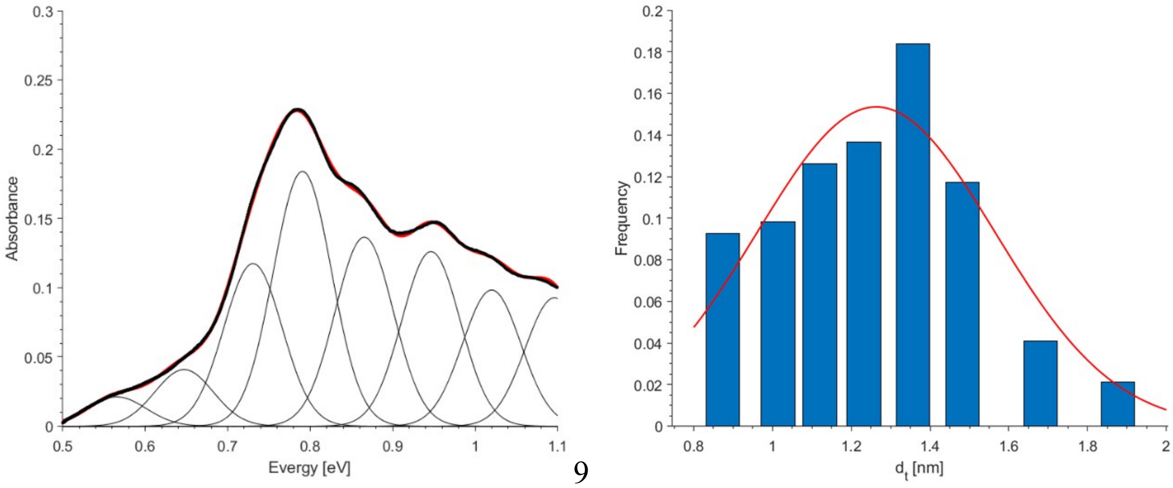

Fig. S1. Absorbance peaks fitted as a sum of gaussian lines after background subtraction in the S_{11} region and calculated diameter distribution. The absorbance is modelled as: $A(E) = \sum_i w_i \exp\left[-\left(\frac{E - E_i}{50\ meV}\right)^2\right]$ [3]. The fit parameters are given in Table S1.

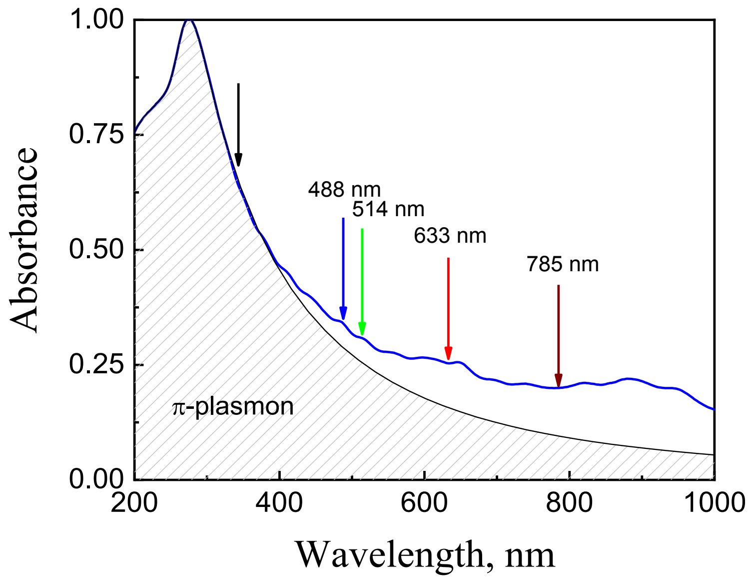

Fig. S2. Decomposition of the optical absorbance spectrum of the SWCNTs. The π-plasmon peak was approximated by a non-linear fit around the position indicated by the black arrow [4]. Fit: $y = ax^b$ with $a = 5 \cdot 10^5 \pm 4.6 \cdot 10^4$, $b = -2.32 \pm 0.06$. The peaks due to electronic transitions in the nanotubes were obtained by subtracting the π-plasmon peak from the total absorbance. The colored arrows indicate the four illuminating laser wavelengths.

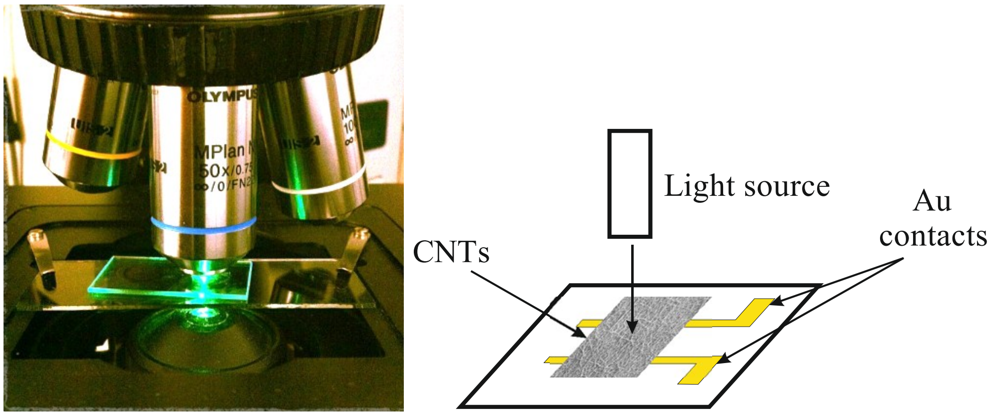

Fig. S3. Image and schematic drawing of the Raman spectrum and two-point capacitance measurement setup. The SWCNT layer is transferred on a glass substrate with parallel contact electrodes and illuminated by a laser.

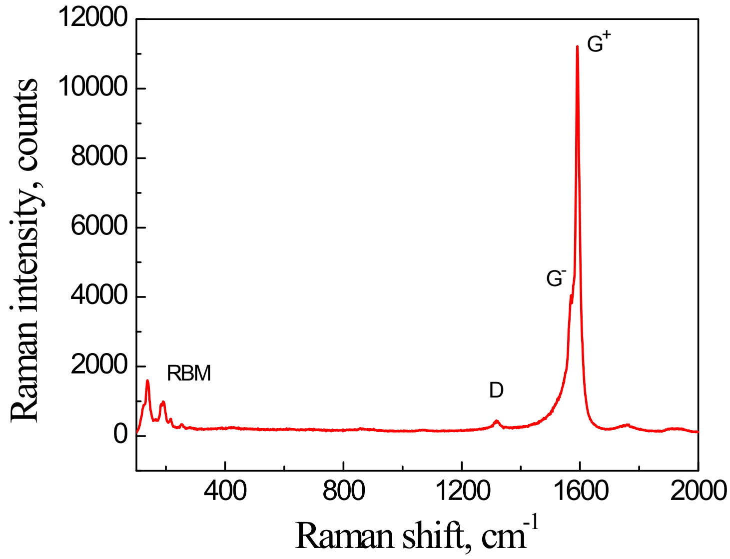

Fig. S4. Raman spectrum of the SWCNT sample with RBM, D, and G peaks highlighted.

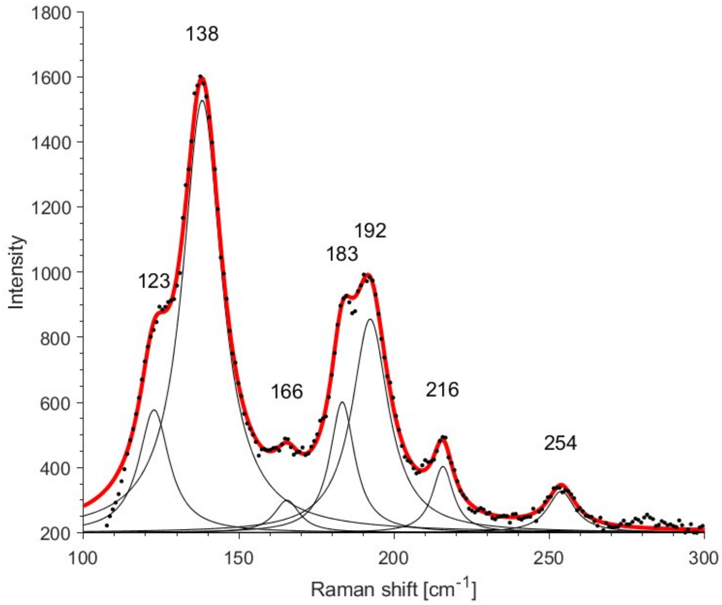

Fig. S5. Decomposition of the RBM peaks in the Raman spectrum of SWCNTs with Lorentzian curves. The fit parameters are given in Table S3.

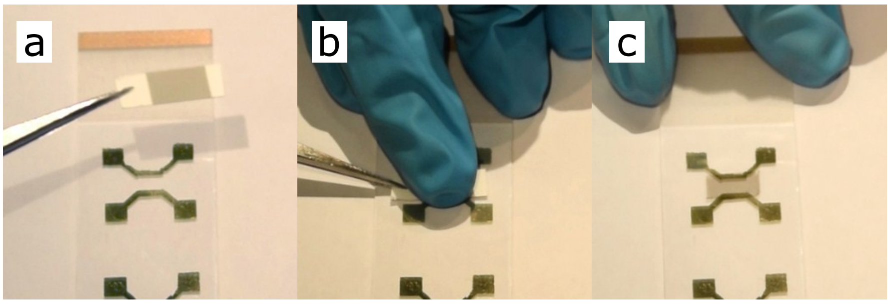

Fig. S6. Dry transfer method of the SWCNT layer [5].

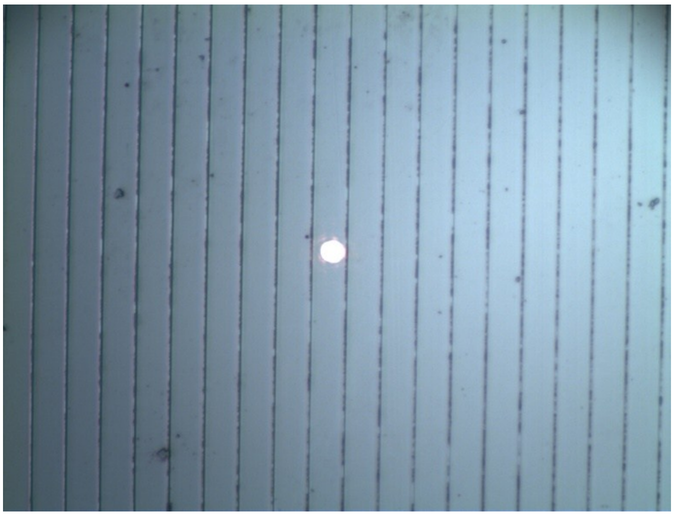

Fig. S7. Determination of the laser spot size with a 10 µm ruler under optical microscope.

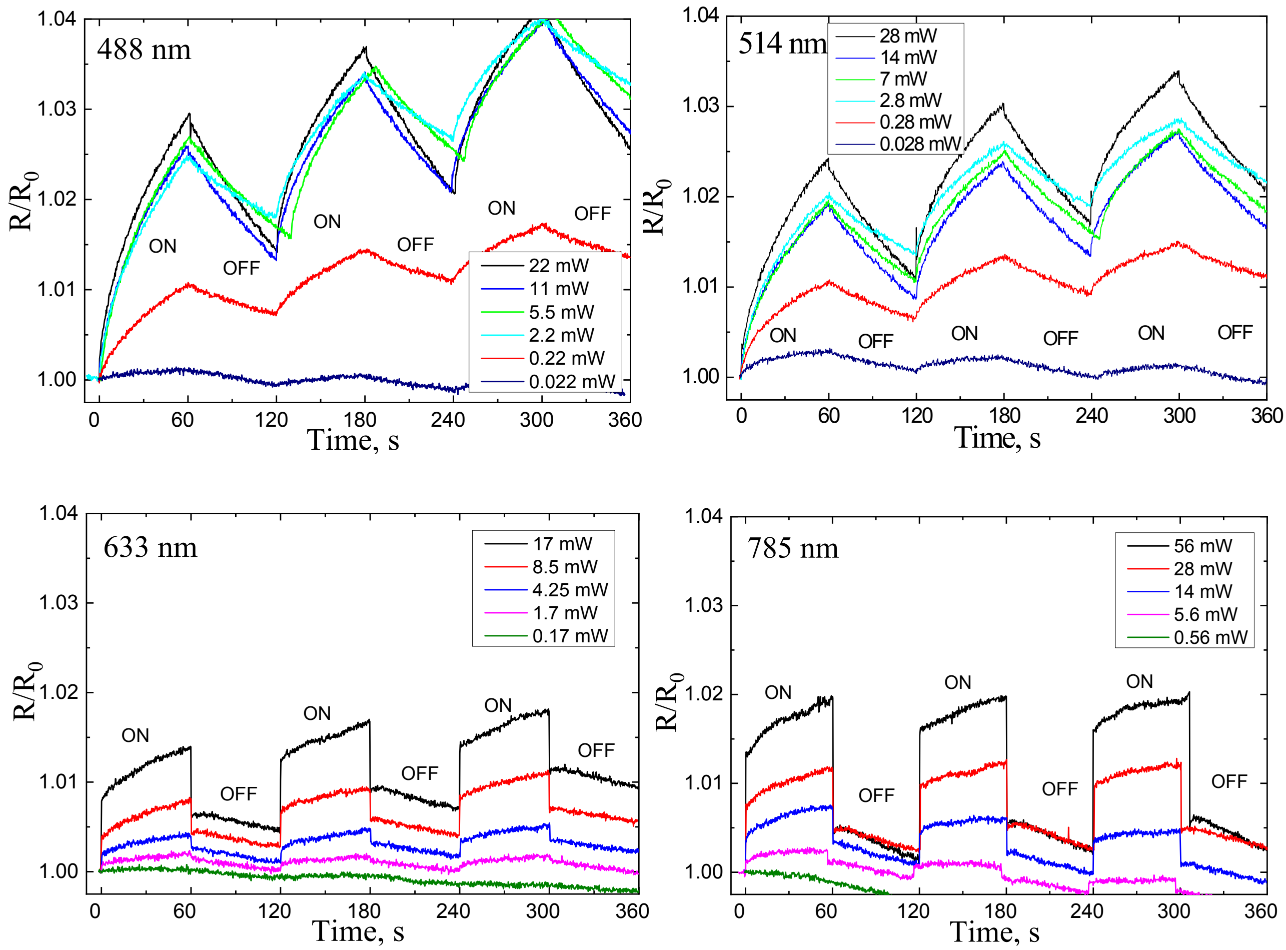

Fig. S8. Change of the SWCNT layer's four-point resistance during illumination with four laser wavelengths and varying power levels. The labels indicate one minute ON and OFF illumination cycles.

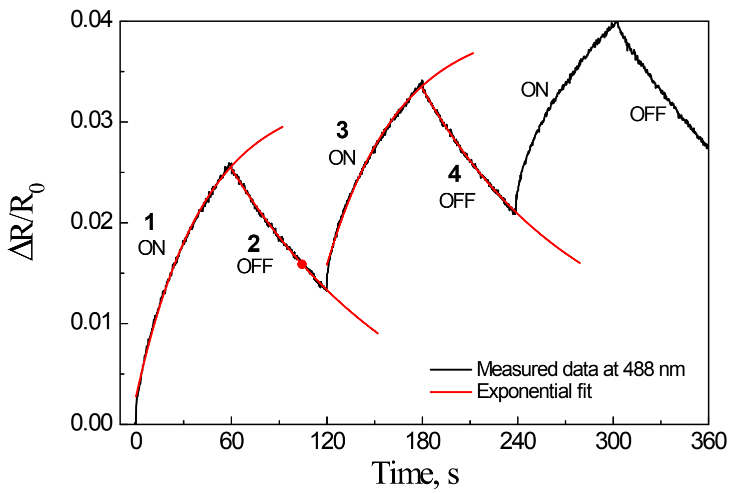

Fig. S9. Evolution of the SWCNT layer's resistance during laser illumination with a wavelength of 488 nm and a power of 11 mW. The labels indicate one minute ON and OFF illumination cycles. The first four cycles **1-4** are fitted by an exponential of the form: $y = y_{0,i} + A_i \cdot \exp(-x/t_i)$. Fit parameters:

$y_{0,1}$ = 0.033, A_1 = -0.03, t_1 = 42.43±0.68;

$y_{0,2}$ = -0.0047±0.0012, A_2 = 0.05, t_2 = 117.65±6.09;

$y_{0,3}$ = 0.04, A_3 = -0.34±0.02, t_3 = 45.24±0.98;

$y_{0,4}$ = 0.006±0.0015, A_4 = 0.17±0.01, t_4 = 98.50±7.23.

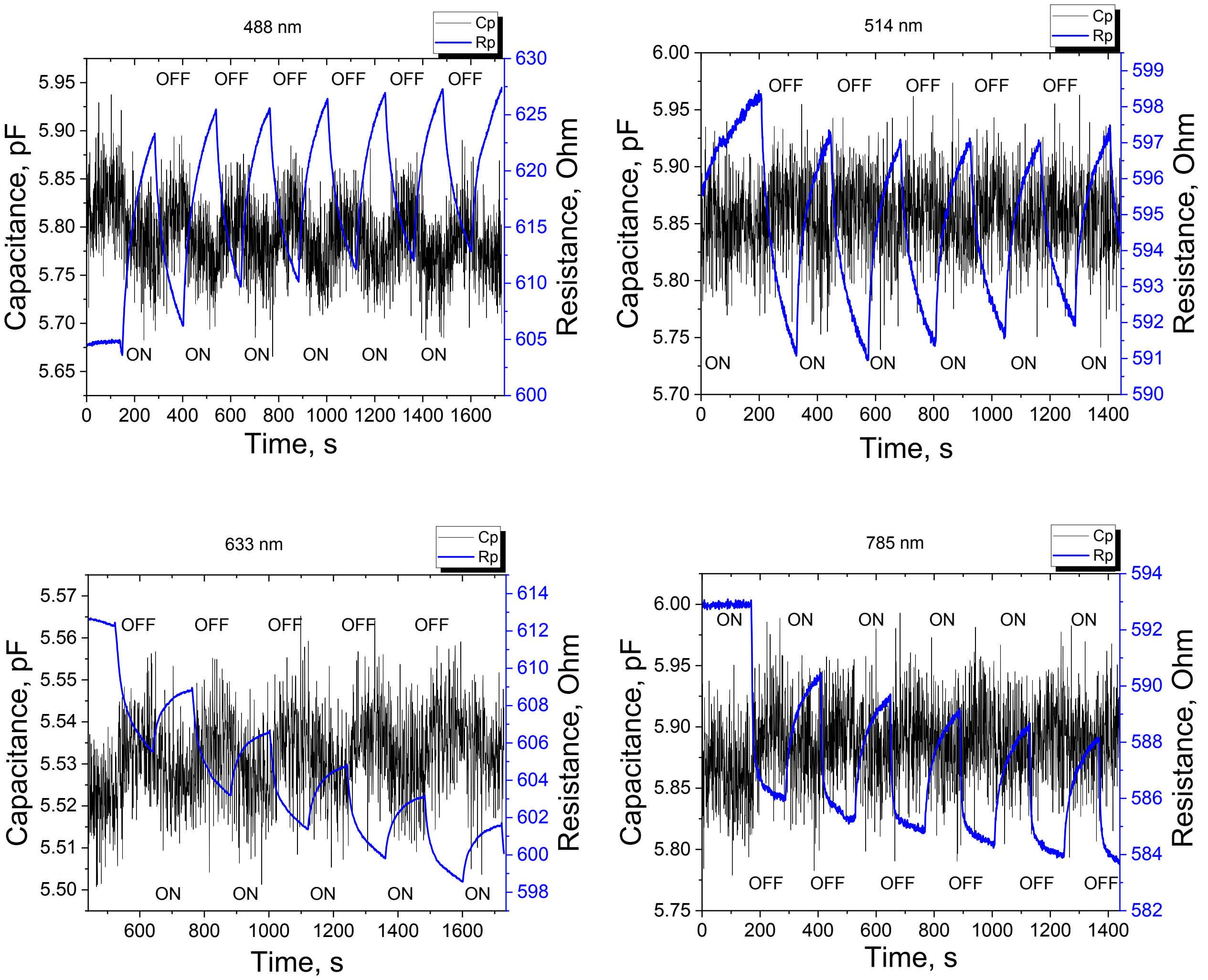

Fig. S10. Change of the SWCNT layer's two-point impedance during illumination with four laser wavelengths and similar power levels. The labels indicate two minutes ON and OFF illumination cycles.

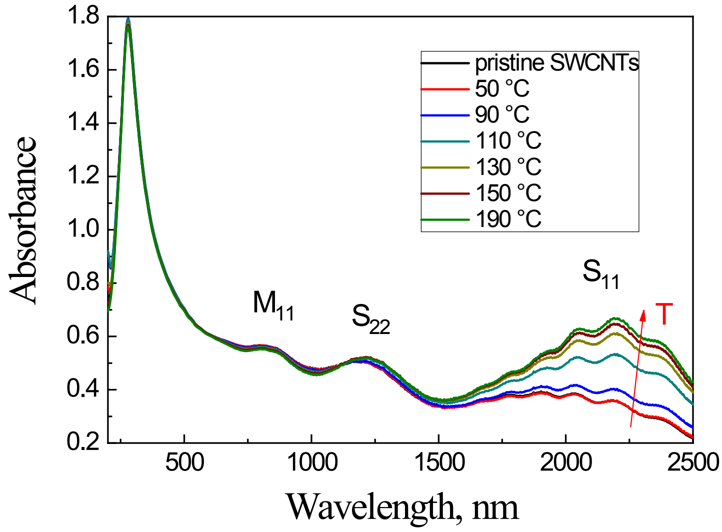

Fig. S11. Effect of heating on the optical absorbance spectrum of SWCNTs.

References

[1] R. B. Weisman and S. M. Bachilo, "Dependence of optical transition energies on structure for single-walled carbon nanotubes in aqueous suspension: an empirical Kataura plot," *Nano Letters,* vol. 3, no. 9, pp. 1235-1238, 2003.

[2] P. T. Araujo *et al.*, "Third and fourth optical transitions in semiconducting carbon nanotubes," *Physical Review Letters,* vol. 98, no. 6, Feb 9 2007.

[3] Y. Tian *et al.*, "Analysis of the Size Distribution of Single-Walled Carbon Nanotubes Using Optical Absorption Spectroscopy," *Journal of Physical Chemistry Letters,* vol. 1, no. 7, pp. 1143-1148, Apr 1 2010.

[4] N. Nair, M. L. Usrey, W.-J. Kim, R. D. Braatz, and M. S. Strano, "Estimation of the (n,m) Concentration Distribution of Single-Walled Carbon Nanotubes from Photoabsorption Spectra," *Analytical Chemistry,* vol. 78, no. 22, pp. 7689-7696, 2006.

[5] S. Smirnov *et al.*, "Optically Controlled Dielectric Properties of Single-Walled Carbon Nanotubes for Terahertz Wave Applications," *Nanoscale,* vol. 10, no. 26, pp. 12291-12296, 2018.